Energy Conversion and Management: X 18 (2023) 100368

Contents lists available at ScienceDirect

Energy Conversion and Management: X

journal homepage: www.sciencedirect.com/journal/energy-conversion-and-management-x

Techno-economic study of Power-to-Power renewable energy storage based on the smart integration of battery, hydrogen, and micro gas turbine technologies

Antonio Escamilla *, David Sánchez, Lourdes García-Rodríguez

University of Seville (Department of Energy Engineering), Camino de los Descubrimientos s/n, Spain

ARTICLE INFO

Keywords:
Power-to-Power
Micro-gas turbines
Renewable hydrogen
Energy storage systems

ABSTRACT

This paper deals with the integration of a Power-to-Power Energy Storage System (P2P-ESS) based on a hydrogen driven micro gas turbine (mGT) for an off-grid application with a continuous demand of 30 kW_e for three European cities: Palermo, Frankfurt, and Newcastle. In the first part of the analysis, the results show that the latitude of the location is a very strong driver in determining the size of the system (hence footprint) and the amount of seasonal storage. The rated capacity of the PV plant and electrolyzer are 37%/41% and 58%/64% higher in Frankfurt and Newcastle, respectively, as compared to the original design for Palermo. And not only this, but seasonal storage also increases largely from 3125 kg H_2 to 5023 and 5920 kg H_2. As a consequence of this, $\overline{LCOE}$ takes values of 0.86 €/kWh, 1.26 €/kWh, and 1.5 €/kWh for the three cities, respectively, whilst round-trip efficiency is approximately 15.7% for the three designs at the 3 cities. Finally, with the aim to reduce the footprint and rating of the different systems, a final assessment of the system hybridised with battery storage shows a 20% $\overline{LCOE}$ reduction and a 10% higher round-trip efficiency.

1. Introduction

The option to store large amounts of energy has been unattainable in the past and it still poses numerous technical challenges nowadays. Given the current quest for an increasing share of renewable energy sources (RES) and the new regulatory framework and social concern for decarbonisation, it is of utmost importance to find affordable, secure, and sustainable energy storage solutions. Power-to-Power (P2P) energy storage systems (ESS) have received a lot of attention in the last years due to the different national plans to develop the supply chain of hydrogen and other alternatives decarbonised fuels [1–4]. Furthermore, due to the large uncertainty and volatility of the energy market in the last years, governments are accelerating the introduction of RES along with the deployment of energy storage options in order to achieve higher security of supply (i.e., energy independence) in line with the Green Deal vision. The European Commission has adopted the "Fit for 55" legislative package [5] which aims at reviewing and adapting the regulatory framework needed to meet the decarbonisation targets for 2030 and 2050.

A P2P-ESS uses surplus electricity from RES to feed an electrolyzer where the splitting of the water molecule yields H_2 and O_2. The H_2 produced is then stored for later utilization to drive a power generation system. Thus, the consumption of originally non-dispatchable renewable electricity is shifted with respect to production, therefore covering the electric demand at any time. In particular, when there is a need for power again, hydrogen can be used to run, for instance, fuel cells and gas turbines, foreseen as the main technologies to dispatch power using H_2. In the current study, focused on decentralised applications, a micro-gas turbine mGT is considered.

The paper deals with the integration of a P2P-ESS based on a mGT (Fig. 1) at different geographical locations. An off-grid application is considered, with a constant demand for 30 kW_e throughout the year (which can be provided by either a PV installation or the storage system). For these scenarios, techno-economic studies have been carried out with a time-step of one hour to understand the sizing of each system and the footprint associated, as well as the Levelized Costs of Hydrogen (LCOH) and Energy (LCOE). Next, hybridization of the P2P-ESS with a battery energy storage system BESS (Fig. 2) is assessed, with the aim to look for options that would decrease the hydrogen demand, thereby decreasing the need for seasonal storage and, accordingly, the footprint

* Corresponding author.
E-mail address: a.escamilla@us.es (A. Escamilla).

https://doi.org/10.1016/j.ecmx.2023.100368

Available online 14 March 2023

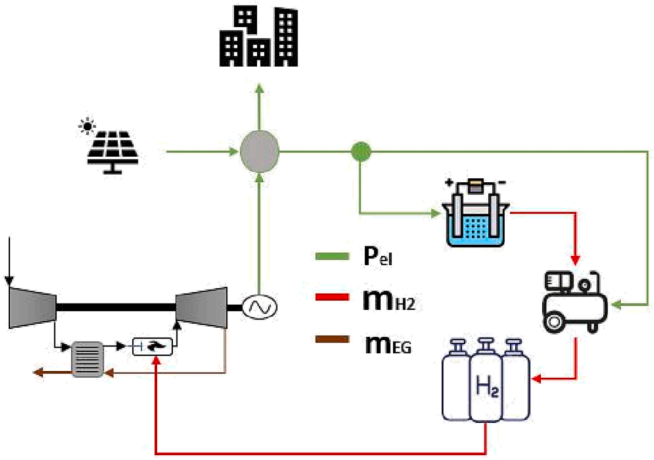

Fig. 1. Layout of the Power-to-Power energy storage system based on micro-gas turbines. P_{el} stands for exchange of electric power and m_{H_2} and m_{EG} stand for streams of hydrogen, and exhaust gases, respectively.

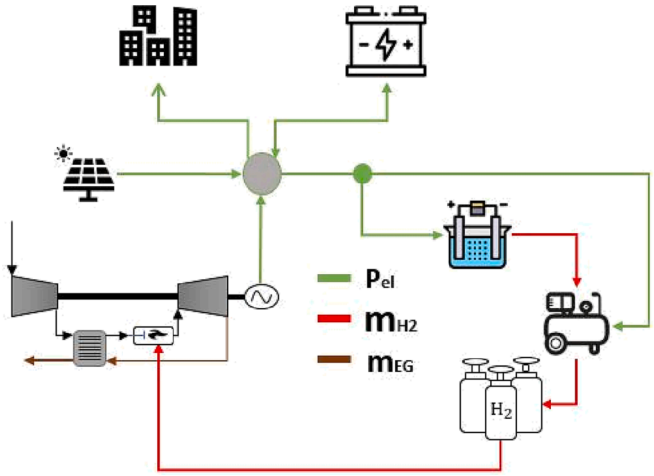

Fig. 2. Power-to-Power energy storage system based on the integration of micro-gas turbine and battery energy storage system layout. P_{el} stands for exchange of electric power and m_{H_2}, and m_{EG} stand for streams of hydrogen, and exhaust gases, respectively.

of the PV solar field and electrolyzer systems. An optimization based on the NSGA-II solver [6] has been carried out to determine the battery bank capacity, the number of PV panels and the number of electrolyzer cells to minimise the LCOE and the surplus energy. All these models are embedded in a software tool coded in Python, which deals with the energy balance, calculation of economic parameters, and optimization of the system design.

This paper aims to contribute to understanding the sizing and operation of a P2P-ESS when is operated in an off-grid application at different sites that owns low, medium, and high global horizontal irradiance (GHI). In addition, in the second part of the paper, hybridization of the P2P-ESS with a BESS is proposed and compared with the base-case scenario. The overarching motivation of the paper is hence to present a techno-economic assessment of this specific ESS which can provide relevant techno-economic information as a function of location and other system features and specifications. Furthermore, this study is a step forward on an already published journal article by the authors [7] in which a market research was conducted to determine the round-trip efficiencies of different P2P layouts with mGTs but without any economic data. Table 1 drafts the main differences between the articles.

In addition, a large number of studies dealing with Power-to-X ESS must be also acknowledged. Heyman et al. [8] use figures of merit for plant size, energy conversion technology, configuration, and cost structure to compare the performance of power-to-gas sites. Also, Loisel *et al.* [9] present an economic evaluation to estimate the LCOH for different scenarios in France but without any thermodynamic analysis. Antonio Escamilla *et al.* [7] present a thermodynamic analysis of different options for the different systems in a P2P-ESS using mGTs to evaluate the round-trip efficiency (RTE) but without economic analysis. Nikolaos Skordoulias *et al.* [10] present a techno-economic evaluation of mid-scale power-to-hydrogen-to-CHP, focusing on the values of LCOH and capacity factor (CF) that would eventually yield an appealing business case for the ESS replacing CH_4. Other authors have looked into P2P-ESS integrated with BESS. Crespi *et al.* [11] compare the use of hydrogen-based P2P systems, battery systems and hybrid hydrogen-battery systems to supply a constant 1 MW_e with electricity generated locally by a photovoltaic plant. Yang Zhang *et al.* [12] perform a comparative study of hydrogen storage and BESS in grid-connected PV systems, focusing on the operational strategy of the system in different operating modes and scenarios. Zaib Shahid *et al.* [13] carry out a techno-economic feasibility analysis of P2P-ESS for small French islands, considering fuel cells as prime movers. The authors report an average LCOE of 0.42 €/kWh when combining hydrogen and BESS. David Parra *et al.* [14] perform a simulation of battery and hydrogen technologies for renewable energy management in a single grid-connected house in the UK. The work shows an increase in the local use of PV energy generated on-site: 171% and 159% for the battery and hydrogen systems, respectively. The aforecited papers share common features with the work presented in this manuscript, to some extent. Nevertheless, there are also major differences. Firstly, as far as the authors know, this is the first time mGTs are considered in P2P-ESS (fuel cells are the usual technology of choice). Secondly, the current study is focus not only on thermodynamic and economic features but also on the feasibility to install such a system under certain boundary conditions, bearing in mind the footprint of the different systems and other specific characteristics that may apply in certain locations. Thirdly, the consequences of seasonal storage, which has been found to increase LCOH substantially, are not considered in any of the studies found by the authors. Table 1 summarises the main

Table 1
Comparison between authors' article. An "X" indicates that the particular article covers the subject described in the first column of the table.

Subject	Actual	[7]	[8]	[9]	[10]	[11]	[12]	[13]	[14]
Market Research		X		X					
Round-Trip Eff. Analysis	X	X	X		X	X		X	X
Power-to-Power system	X	X		X	X	X	X	X	X
Location Dependency	X		X					X	
Detailed Mathematical Modeling	X			X			X		
Hourly Energy Balance	X			X		X	X		X
BESS	X					X	X	X	X
mGT	X	X							
Optimization	X					X	X	X	
LCOE & LOCH	X			X	X	X	X	X	X
Seasonal Storage Analysis	X								

differences between the articles.

The paper is organised as follows. Section 1 provides a comprehensive literature review of techno-economic studies that have considered P2P-ESS relying on different technologies. Section 2 presents the mathematical and performance models for each of the systems considered. Section 3 presents the methodologies for the calculation of the LCOH and LCOE along with the economic metrics to assess the latter. Section 4 starts with a techno-economic study of the P2P-ESS for three different cities around Europe. Finally, Section 5 considers the hybridization of P2P-ESS with a BESS. Conclusions are shown in Section 6.

2. System description and modelling of P2P-ESS

This section describes the methodology followed to determine both the size and energy balance for each system involved in the P2P-ESS unit. To this end, the interconnection between the different systems is described first, followed by the mathematical modelling used for each system. The following assumptions apply to the design of the P2P-ESS:

- The systems are designed to meet the electrical demand.
- Power demand is given priority over hydrogen production.
- Heat demand is null.
- The power rating of the electric demand is set to 30 kW_e continuously.
- Off-grid application.
- The time-step of calculations is set to 1 h.
- Hydrogen is stored at a pressure of 400 bar.
- The pressure ratio of the H_2 compressor is constant.
- Vessel H_2 leakage is considered null.

Fig. 1 shows the energy flow within the P2P-ESS. Energy production from RES is first used to meet the end-user demand for electricity. In the case of surplus energy, this is used to operate a Proton-Exchange Membrane Electrolyser (PEMEC) to produce H_2 which is stored in high-pressure vessels using a set of reciprocating compressors. In periods when RES is not sufficient to cover the electric demand of the end-user, this stored hydrogen is used to run a micro-gas turbine (mGT) which makes up for the lack of electricity coming from the PV field. This describes the base-case scenario, whose layout is later enhanced through the addition of batteries with the aim of lowering the Levelized Cost of Energy (LCOE) and the footprint of the system. Fig. 2 shows the layout of this second case.

In order to assess the differences that can be obtained from the techno-economic analysis, both from a sizing and economical point of view, the P2P-ESS systems are evaluated at geographical locations that satisfy the following global horizontal irradiance (GHI) criteria,

- City 1: GHI $>$ 4.5 kWh/m^2/day
- City 2: 3 $<$ GHI $<=$ 4.5 kWh/m^2/day
- City 3: GHI $<=$ 3 kWh/m^2/day

In order to carry out a concrete techno-economic analysis, a specific location has been chosen for city 1, 2 and 3 which meets the previous criteria. Thus, Palermo (IT), Frankfurt (GE), and Newcastle upon Tyne (UK) have been chosen. The GHI is 4.73, 3.26, and 2.75 kWh/m^2/day for the three locations, respectively.

2.1. Solar photovoltaic plant

The open-source software System Advisory Model (SAM) developed by the National Renewable Energy Laboratory NREL [15] is used for the modelling and design of renewable energy sources. It is a performance and financial model software tool able to estimate system performance and cost of energy for grid-connected power projects based on installation/operating costs and on system design parameters set by the user.

Table 2 summarizes the main input parameters needed to model the performance of photovoltaic systems. It is worth highlighting that SAM is only used in this work to estimate the performance of renewable energy sources whereas the financial model to calculate LCOE is directly implemented in the software developed by the authors. Once the calculations are completed, SAM provides a wide selection of results which can be retrieved on either hourly, monthly or yearly basis. More information about SAM can be found in [15].

Table 2
SAM photovoltaic solar sections and parameters.

Section	Description
Location and Resource	This information is given by a file which owns all the information about the location and solar resource of a particular place over a year.
Module	For each time step of the simulation, the module model calculates the DC electrical output of a single module based on the design parameters and the incident solar radiation calculated from data in the weather file.
Inverter	Several models to represent the inverter performance model and either choose an inverter from a list, or enter inverter parameters from a manufacturer's data sheet using either a weighted efficiency or a table of part-load efficiency values.
System Design	Use the System Design variables to size the photovoltaic system and choose tracking options. Number of inverters, DC to AC ratio, Subarray 1 Configuration are some of the parameters which need to be decided in this section.
Losses	Loss inputs account for soiling and electrical losses that the module and inverter models do not account for.

SAM has a dedicated Python package, PySAM [16], which can be called from a Python code to carry out SAM simulations and access SAM's default values and input variables. PySAM is a wrapper around the SAM library that groups the C API functions into modules either by technology or financial models.

The solar panel and configuration that have been chosen remain for each scenario and case and so are the losses that are applied. The values of these parameters are shown in Table 3. Irradiation data for each of the locations have been obtained from the European Commission JRC's Photovoltaic Geographical Information System (PVGIS) [17].

2.2. Battery energy storage system

The BESS considered in this study is to be *behind-the-meter* and DC-connected, as shown in Fig. 3. The battery of choice is of the Lithium-ion type and the corresponding performance is modelled as in DiOrio *et. al* [18]. This latter model is actually simplified to account for charging and discharging losses only.

In order to design the BESS, the nominal bank capacity and power and the depth of charge/discharge are specified. In addition, the charging/discharging efficiency determines the round-trip efficiency of the BESS. The following equations apply:

$$C - rate_{disch} = \text{Max. Discharge Power/Bank Capacity}$$

$$C - rate_{char} = \text{Max. Charge Power/Bank Capacity}$$

Table 3
Solar PV design parameters.

Parameter	Unit	Value
Module brand	-	SunPower
Module model	-	SPR-a410-COM
Module max. power	W_{DC}	448.4
Module eff.	%	22.09
Tilt	deg	30
Azimuth	deg	180
Total DC loss	%	4.44
Total AC loss	%	1
Soiling loss	%	5

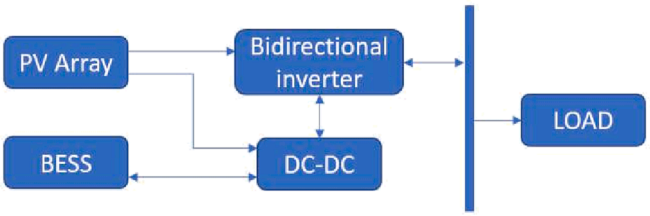

Fig. 3. BESS Layout (Behind-the-meter and DC-connected).

$t_{max.power}$ = Bank Capacity/Max. Bank Power

Table 4 shows the design parameters that have been chosen for the BESS. In this case, the charging/discharging efficiencies have been set to 90%, slightly lower than current state-of-the-art in order to account for the losses that are not considered in the modelling. Additionally, the bank power has been sized to 30 kW so that the BESS can supply the application's energy demand self-sufficiently, without needing the support of the mGT system. Hence, once the BESS runs out of energy, the mGT starts up to satisfy the energy demand until the PV solar field starts producing energy again. The minimum and maximum State-of-Charge (SoC) are set to 20% and 90% respectively, to prevent a high degradation rate of the battery. Finally, a bank power range is specified since this parameter will later be optimised in Section 5. The range considers a minimum duration of 4 h and a maximum duration of 13 h.

2.3. Proton-exchange membrane electrolyser

Polarization curves are a common tool to model the performance of electrolyzers. These do not hold detailed information; however, they are standard performance estimates and one of the most common methods of testing electrolyzer cells since they allow for easy comparison against other polarisation curves. The polarization curve displays the voltage output of the electrolysis cell for a given current density. Polarization curves can be obtained experimentally with a potentiostat/galvanostat, which draws a fixed current from the electrolysis cell and measures the electrolysis cell output voltage. By slowly "stepping up" the load, the voltage response of the electrolyzer cell can be determined. Hence, the polarization curve provides a voltage that depends on operating conditions such as temperature, pressure, applied load, and fuel/oxidant flow rates. It determines the minimum voltage that needs to be applied at a specific load for water electrolysis to take place.

The actual voltage to be applied to the electrolyzer cell is actually higher than the theoretical model due to activation, charge and mass transfer losses. The performance of an electrolyzer can be illustrated using a polarization curve that can be broken into three contributions/sections: (1) activation loss, (2) ohmic loss, (3) mass transport loss. All these voltage losses need to be added to the reversible voltage, or the theoretical minimum voltage for the electrochemical reaction to develop when all other losses are neglected:

$$V = V_{ocv} + V_{act} + V_{diff} + V_{ohm} \quad (1)$$

where V_{ocv} is the open circuit overpotential as well as the theoretical minimum voltage for PEM electrolyzer cells (when neglecting other overpotentials), V_{act} is the overpotential due to the activation energy of the electrochemical reaction, V_{diff} is the diffusion overpotential brought about by limited mass transport in the electrolyzers, and V_{ohm} is the ohmic overpotential caused by the resistance of the electrolyzer cell to the flow of ions/electrons.

The focus of this paper is not to treat the modelling of the electrolyzer cell in detail; therefore, the polarization curve of the electrolyzer is calculated using Eq. (1). Details about the thermo-chemical modeling are discussed in previous works by the authors [19]. It is worth highlighting that the diffusion overpotential is considered null in this analysis since it is only relevant at high current densities, which is not the case in the application considered in this work [20].

The aforedescribed model is used in this work to determine the polarization curve of a specific PEMEC, which is not affected by the number of cells and stacks. An examplary polarization curve for the design parameters summarized in Table 5 is shown in Fig. 4. This input data remains constant for all scenarios and cases.

2.4. High Pressure H_2 Storage

This section describes a thermodynamic analysis of the compression system. This process can initially be assumed to be comprised of an isentropic compression with intercooling, in order to resemble a quasi-isothermal process with lower compression work.

It is assumed that the pressure delivered from the compressor is always the target storage pressure, regardless of the amount of hydrogen stored in each tank. This is, however, not true in practice since the pressure delivered by the compressor must be slightly higher than that of the tank, the difference being Δp at each time step. Hence, this pressure-balance is a conservative assumption that allows the decoupling of the refilling process from the number of vessels and their filling status. Regarding the reciprocating compressor, a previous work by the authors provide detailed information about the models used [19] and the assumptions made.

Regarding the geometry and specifications of the vessel, this is designed according to ASME Section VIII, Division 1, 2, or 3 [22]. The design of such vessels can be divided into shell and head. Each of these can be of different types, such as cylindrical or spherical shells, ellipsoidal, or torispherical heads; moreover, the dimensions and design of each of these parts are different depending on whether they experience internal or external pressure. In this work, all equations and criteria exposed below belong to "under internal pressure" and can be seen in Table 6. The minimum wall thickness (t) depends mostly on the design internal pressure (P) and internal radius (R) of the vessel, and on the allowable stress (S) and joint efficiency (E) of the material. In the case of the vessel's head, the radius is not a valid measure anymore and the inside diameter of the head skirt (D) or the inside crown radius (L) is used.

In the case of the compression system, the following parameters are used to determine the (hydrogen) compressor and (cooling water) pump work (W_{comp}, W_{pump}):

- n_{stages} is the number of stages,
- $\dot{m}_{H_2}$ and $\dot{m}_{H_2O}$ are the mass flow rate of hydrogen and cooling water [kg/s],
- h_1 and h_2 are the inlet and outlet specific enthalpies of each stage [kJ/kg-K],

Table 4
BESS design parameters.

Parameter	Unit	Value
Bank Power	kW	30
Bank Capacity	kWh	(120, 400)
Min. State-of-Charge	%	20
Max. State-of-Charge	%	90
Charge/Discharge Eff.	%	90

Table 5
PEMEC design parameters.

Parameter	Unit	Value
Current Density Range	A/cm^2	0.2–2.0
Auxiliary Power	%	10
Cell Area	cm^2	160
Cathode Temperature	°C	50
Cathode Pressure	bar	30

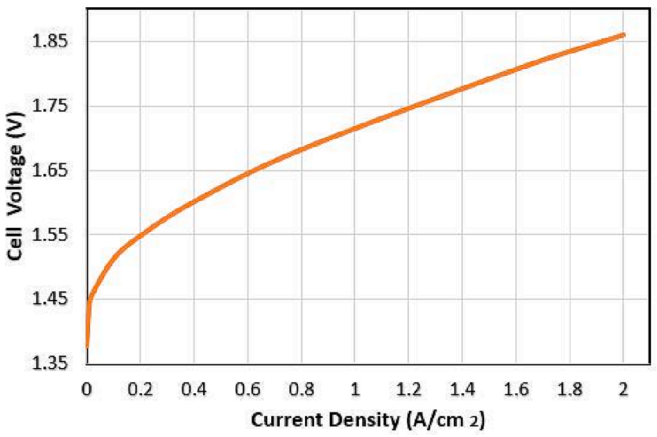

Fig. 4. PEMEC polarization curve. Validated against experimental data shown in [21].

Table 6
Summary of equations for the storage system modelling.

Tank dimensions	Compression system
Cylindrical Shell: $t = \frac{PR}{2SE - 0.2P}$	$W_{comp} = \dot{m}_{H_2} - + \sum_{i=1}^{n_{stages}} (h_2 - h_1)_i$
Spherical Shell: $t = \frac{PR}{2SE - 0.2P}$	$h_2 = f(T_2, P_2);\ T_2 = f(\eta_{pol}, PR_i)$
Ellipsoidal Head: $t = \frac{PD}{2SE - 0.2P}$	$W_{pump} = n_{stages} - + \frac{g - + H - + \frac{\dot{m}_{H_2O}}{\dot{m}_{H_2}}}{\eta_{pump}}$
Torispherical Head: $t = \frac{0.885PL}{SE - 0.1P}$	$\frac{\dot{m}_{H_2O}}{\dot{m}_{H_2}} = \frac{h_{1_{H_2}} - h_{2_{H_2}}}{h_{2_{H_2O}} - h_{1_{H_2O}}}$
Hemispherical Head: $t = \frac{PL}{2SE - 0.2P}$	

- P_2 and T_2 are the outlet pressure and temperature of each compressor stage [bar, K],
- PR_i is the stage pressure ratio for each compression stage,
- η_{pol} is the politropic efficiency of each compressor stage,
- η_{pump} is the isentropic efficiency of the pump,
- H_i is the head of the pump [m] for each of the intercooling stages,
- g is the gravitational acceleration, estimated at 9.81 [m s^{-2}].

The values of the parameters that have been used for the design of the high-pressure vessel and compression system are listed in Table 7. It is assumed that the outlet temperature for each compressor stage cannot be higher than 420 K [23] and that the pressure ratio between the hot and cold sides of the intercooler is 10. The latter facilitates the calculation of the work done by the water pump and determines the maximum pressure ratio that the heat exchanger must endure. This criterion is set to determine the number of stages that the reciprocating compressor must have to deliver a pressure ratio of 13.33.

Table 7
H_2 storage design parameters.

Parameter	Unit	Value
Inside Radius	cm	0.4
Shell Length	cm	1.87
Joint Efficiency Factor	-	1
Material Allowable Stress	MPa	55
Material Density	kg/m^3	2000
Final Storage Pressure	MPa	40
Compressor Isentropic Eff.	%	75
Compressor Max. Outlet Temp.	K	420
Pump Isentropic Eff.	%	90
Cooler fluid	-	Water
Cooler Inlet/Max. Outlet Temp.	K	293/363

2.5. Micro gas turbine

The current section describes the thermodynamic modelling that is adopted for the mGT. Using in-house software developed at the University of Seville, the off-design maps of the compressor and turbine are obtained. Considering a minimum turndown capability of 20%, the running line of the mGT is found by merely matching the off-design performance of turbomachines on the same shafts. In this regard, the methodology explained below corresponds to a single-shaft, recuperative gas turbine [24] whose off-design performance comes determined by the interaction of engine components: namely, compressor, turbine, combustor, and recuperator.

Off-design performance of rotating machinery in a micro gas turbine is usually represented by non-dimensional characteristics for the variation of temperature, pressure, mass flow rate, and speed, whilst isentropic efficiency is the metric for process reversibility. The correct definitions of these non-dimensional parameters are as follows, assuming the gas behaves ideally:

$$\text{Non} - \text{dimensional flow} = \frac{m_1\sqrt{R_1 T_1/\gamma_1}}{D^2 P_1} \tag{2}$$

$$\text{Non} - \text{dimensional speed} = \frac{N_1}{\sqrt{\gamma_1 R_1 T_1}} \tag{3}$$

$$\text{Pressure ratio} = P_2/P_1 \tag{4}$$

where m_1, T_1, P_1 and D are the inlet mass flow rate, temperature, pressure, and reference diameter of the compressor or turbine, respectively, and N_1 is the rotational speed of the compressor or turbine. P_2 is the discharge pressure of the compressor or turbine and R_1 and γ_1 are the gas constant and isentropic index. Figs. 5 and 6 show the off-design performance of the compressor and turbine in terms of corrected mass flow rate and pressure ratio; efficiency islands are also shown.

The matching process between compressor and turbine considers that the pressure losses at the inlet (to the compressor) and outlet (from the expander) are null, and that the absolute mass flow rate through the compressor and turbine are equal (i.e., hydrogen mass flow rate is much lower than that of air). The process to find the new operating conditions in off-design is as follows:

- Step 1: Specify turbine inlet temperature (T_5), gas turbine speed (N_1), compressor inlet pressure (P_1) and temperature (T_1).
- Step 2: Estimate compressor inlet flow (m_1) and pressure ratio (P_2/P_1).
- Step 3: Compressor:
  Step 3.1: Calculate corrected mass flow rate, Eq. (2).
  Step 3.2: Determine corrected speed and isentropic efficiency (η_{12}) from the corrected performance map of the compressor, Fig. 5, using corrected mass flow rate and pressure ratio (P_2/P_1) of the compressor.
  Step 3.3: Calculate compressor outlet temperature (T_2) and power (W_{comp}):

$$T_2 = T_1 + T_1 \Big/ \eta_{12}\left((P_2/P_1)^{\frac{\gamma-1}{\gamma}}\right) \tag{5}$$

$$W_{comp} = m_1 \cdot (h_2 - h_1) \tag{6}$$

  where h_1 and h_2 are the specific enthalpies at compressor inlet and outlet.
- Step 4: Turbine:
  Step 4.1:Calculate of corrected mass flow rate, Eq. . (2).
  Step 4.2:Determine corrected speed and isentropic efficiency (η_{56}) from the corrected performance map of the turbine, Fig. 6, using turbine corrected flow rate and pressure ratio (P_5/P_6).

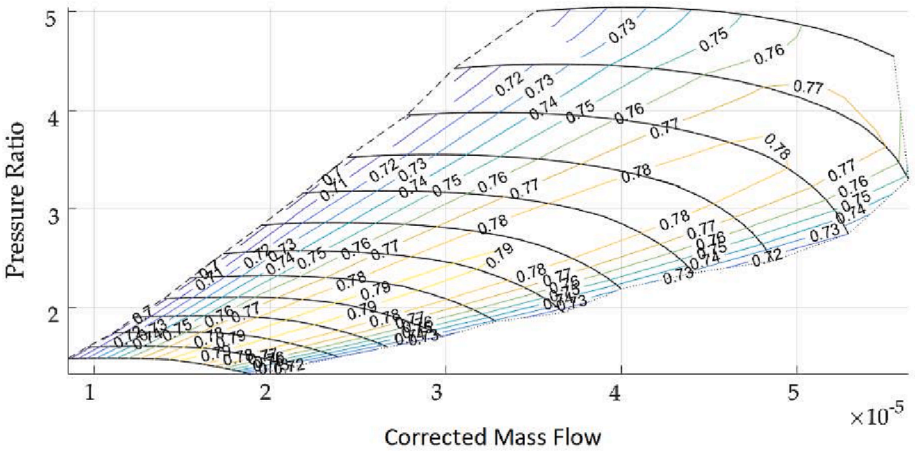

Fig. 5. Corrected compressor map.

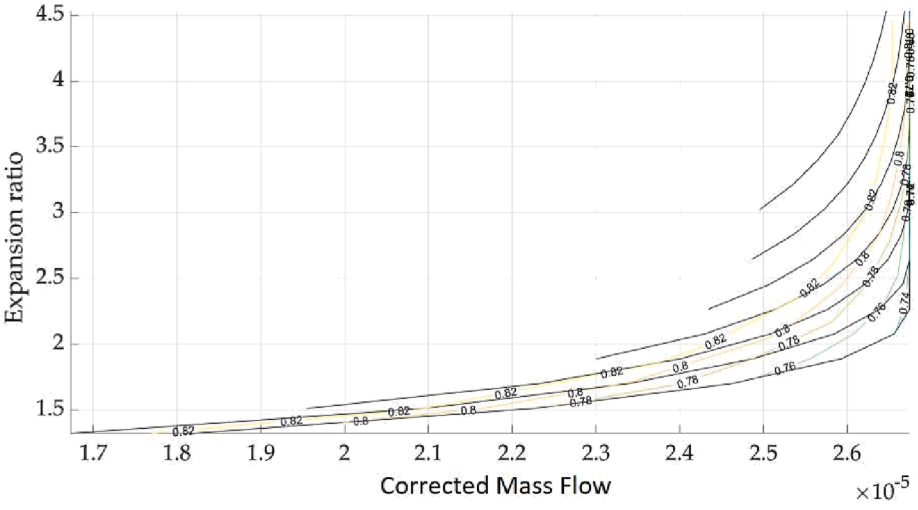

Fig. 6. Corrected turbine map.

Step 4.3:Calculate turbine outlet temperature (T_6) and power (W_{tur}):

$$T_6 = T_5 + T_5 \Big/ \eta_{56}\left(1 - (P_5/P_6)^{\frac{\gamma-1}{\gamma}}\right) \tag{7}$$

$$W_{tur} = m_1 \cdot (h_5 - h_6) \tag{8}$$

where h_5 and h_6 are the specific enthalpies at the turbine inlet and outlet.

- Step 5: Combustor and recuperator:
  Step 5.1:Calculate air temperature at the inlet to the combustor or outlet from the heat-exchanger (T_4).
  Step 5.2:Calculate combustor outlet temperature (T_5):

$$T_5 = T_4 * \frac{1 + \frac{f * \eta_{CC} * LHV_{H_2}}{\overline{c_P} * T_4}}{1 + f} \tag{9}$$

  where f is the fuel-to-air ratio, $\overline{c_P}$ is the average heat capacity between T_4 and T_5, respectively.
- Step 6: Check 1:
  – Step 6.1: Compare the calculated rotational speed of the compressor and turbine. If they are not the same, update m_1. This loop involves steps 3 and 4.
- Step 7: Check 2:
  Step 7.1:Compare the calculated turbine inlet temperature with the set TIT. If they are not the same, update *PR*. This involves steps 3, 4, and 5.

After completing the matching process using Figs. 5 and 6, the performance map of the entire 30 kW_e mGT is shown in Fig. 7. This set of curves is then used to obtain the operating conditions of the mGT at different settings depending on the power demand of the end user. It is worthwhile to mention that the curve has been obtained for an athmospheric temperature of 20 °C. In the case of different atmospheric temperature, step 1 to 7 must be repeated to find the new working mGT curve.

3. Techno-economic analysis of P2P-ESS systems

The current section presents a detailed discussion about the economics of the layout presented in this paper. This economic assessment provides a closure of the techno-economic modelling and assessment that is addressed in the next sections.

An extensive literature review has been conducted to gather the necessary economic information about the systems involved: PV, BESS, PEMEC, H_2-compressor, H_2-tanks, and mGT. Out of this literature review conducted by the authors, the values presented in Table 8 have been chosen for the different systems at each location. It is assumed that

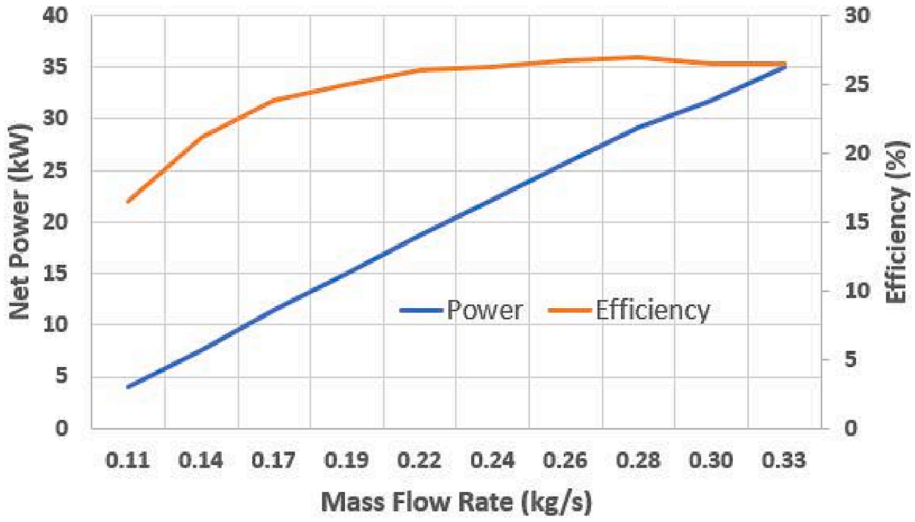

Fig. 7. Off-design curve of the 30 kW_e mGT used in this work.

Table 8
Economic input data for the components of the plant. These data are used to calculate LCOH and LCOE of the P2P-ESS. €refers to 2021.

System	Parameter	Unit	Value [$€_{2021}$]	Reference
PV Solar	CapEx	€/kW	664/587/717	[25]
	Fixed OpEx	€/kW per year	15.4 (OECD)	[25]
	Var. OpEx	€/kWh	0.0	
	Lifetime	year	25	
BESS	CapEx	€/kWh	402.5[1]	[26]
	Fixed OpEx	% of CapEx	2.5	[27]
	Stack Replacement	% of CapEx	40	[26]
	Stack Lifetime	year	15	[27]
PEMEC	CapEx	€/kW	1100[2]	[28,29]
	Fixed OpEx	% of CapEx	1.5	
	Stack replacement	% of CapEx	45	[28]
	Stack lifetime	year	10	
	Water cost	€/m^3	4.9	
Compressor	CapEx	€/kW	4500	[30] [31]
	OpEx	% of CapEx	4	[31]
Vessel	CapEx	€/kg H_2	470	[32]
	OpEx	% of CapEx	2	[32]
mGT	CapEx	€/kW	2689	[33]
	Fixed OpEx	€/kW	150	[34]
General	Interest Rate	%	4	
	Project Lifetime	year	25	

1. Based on a rated output of 1 MW_e and a total storage capacity of 4 h Lithium-Ion BESS.
2. Based on a 500 kW PEMEC.

the costs associated with each technology remain unchanged from one location to another except for the case of the PV plant. For the latter item, the information about regional costs (CapEx and OpEx) of utility-scale PV plants is taken from reference [25].

The LCOE is the average cost of electrical energy produced by a system over its accounting lifetime. For the calculation of LCOE, the capital recovery factor (CRF) methodology is used. CRF is the ratio of a constant annuity to the present value of receiving that annuity for a given period of time. Using the discount rate, *i*, and the accounting lifetime, *N*. Mathematically, the CRF is calculated as follows:

$$CRF = \frac{i}{1 - \frac{1}{(1+i)^N}} \tag{10}$$

LCOE is then defined as:

$$LCOE = \frac{CRF \cdot TCC + FOC}{AEP} + VOC \tag{11}$$

where:

- TCC is the total capital cost, €, or installed capital cost,
- FOC is the fixed annual operating cost, €, or operation & maintenance costs,
- AEP is the annual production of electricity, kWh, and,
- VOC is the variable operating cost, €/kWh, or operation & maintenance costs per unit of annual yield.

Akin to LCOE, LCOH is defined as the minimum value at which hydrogen must be sold for an energy project to break even. Eq. (11) also applies to LCOH. With the information displayed on Table 8, the TCC, FOC, and VOC for hydrogen are calculated as follows:

$$TCC = TCC_{ec} + TCC_{comp} + TCC_{st} \tag{12}$$

$$FOC = TOC_{ec} + TOC_{comp} + TOC_{rep,a} \tag{13}$$

$$VOC = VOC_e + VOC_w \tag{14}$$

where:

$$TOC_{rep,a} = CRF * \frac{TOC_{rep}}{(1+i)^t} \tag{15}$$

where *ec* stands for electrolyzer, *comp* stands for compressor, *st* stands for storage, *rep*, *a* stands for electrolyzer stack replacement, *e* stands for electricity, and *w* stands for water.

4. Base-case scenario: P2P with mGT

This section presents the design of the base-case P2P-ESS layout (Fig. 1). The calculations are performed for 3 different locations (Palermo, Frankfurt, and Newcastle) to understand how the available solar resource impacts the footprint of each system as well as the LCOH

and LCOE of the application. The assumptions and integration layouts of each model presented in Section 2 are incorporated into the in-house software and a detailed analysis of the energy balance for each system is performed at 1 h time steps over a year. The sizing of the ESS is carried out for Palermo and the resulting specifications are then placed in Frankfurt and Newcastle to understand how the location would affect the energy balance and economic parameters of a standardised design. After, the ESS is specifically designed for Frankfurt and Newcastle to understand how the standarised solution must change from a high GHI location to lower GHI locations (Section 4.1).

Weather files for each location have been obtained from the Photovoltaic Geographical Information System (PVGIS) [17] for a typical Meteorological Year (TMY).

As said, the power demand is constant throughout the whole year, 30 kW_e. For this specification, the system is sized for the boundary conditions in Palermo, in order to be able to operate without grid support. In addition to Tables 3, 5, and 7, Table 9 contains a summary of the main design parameters (see Section 2) for the base-case scenario (Fig. 1).

Once the size of the subsystems is determined to meet the end user's requirements, an energy balance of the integrated system is carried out. Table 10 shows the yearly values for the energy balance of the P2P-ESS along with the economic data for LCOH and LCOE. In addition, Fig. 8 shows the hourly energy balance of the power-to-power system over the entire year, an information that is completed by Figs. 9 and 10 for a better understanding. Fig. 9 shows the energy balance of the power-to-hydrogen process: energy yield of the PV panels (red line), power consumed by the electrolyzer (blue line), and the production of hydrogen for each time step (black dots). The significant oversizing of the PV array and the electrolyzer becomes evident. This is mostly due to the low round-trip efficiency of the ESS as well as to the need for a very large production of hydrogen during sun hours in order to compensate for the lack of production during the night. As opposed to this, Fig. 10 shows the hydrogen-to-power process, represented by the load of the mGT, which is operated when renewable energy is not available. It is confirmed that the mGT works at partial load only rarely, what has a strong, positive impact on round-trip efficiency.

Table 10 shows similar information for a system designed in Palermo but operated in Frankfurt and Newcastle. These two locations are in a much more northern latitude than Palermo and, therefore, receive less radiation (W/m^2-year), meaning that the system is not able to fulfil the energy demand of the end-user without grid support. This simple exercise is meant to quantify how much the location of a P2P-ESS does not only affect the footprint of the system but also LCOH and LCOE. For the system designed in Palermo, the net-H_2[1] produced by the end of the year is about 141 kg, whereas hydrogen production decreases considerably due to the lower capacity factor of the solar panels when the same system is installed in either of the other two locations. In particular, for the locations of Frankfurt and Newcastle, the net-H_2 balance at the end of the year in order to satisfy the 30 kW_e is (5247) kg and (7302) kg, approximately, where "()" means a negative value. Fig. 11 shows the hourly evolution of the net hydrogen balance for each location as described before; it is clear that not enough hydrogen is produced during the sunny season to cope with a long winter. Hence, for the sake of economic comparison between the different locations, the same amount of seasonal storage as for the case of Palermo is considered, 3125 kg H_2. This parameter affects how many vessels must be in place to be able to store that amount of H_2.

Figs. 12 and 13 show the resulting LCOH and $LCOE_{mGT}$ for the cities of Palermo, Frankfurt, and Newcastle. Even if it must be acknowledged that the system is designed for Palermo, regardless of the site, it becomes apparent that the much higher costs of producing hydrogen and power in Northern Europe are not due to this reason; actually, the upsurge in energy and hydrogen costs is influenced mainly by the increasing $LCOE_{PV}$ due to the lower radiation and lower capacity factors. In addition, the breakdown of costs associated with LCOH suggests that seasonal storage is the cost that has the largest contribution to the final price of hydrogen, about 50%. This is followed by the installation cost of the electrolyzer (CapEx) and the power consumed by the EC. When the costs associated with compression and storage of H_2 are not considered, the LCOH and $LCOE_{mGT}$ are reduced to 5.19 €/kg H_2 and 0.65 €/kWh, 6.74 €/kg H_2 and 0.82 €/kWh, and 8.22 €/kg H_2 and 0.99 €/kWh, for the cities of Palermo, Frankfurt, and Newcastle respectively. Therefore, it is of utmost importance to include the cost of storing H_2 in the calculation of the LCOE of a P2P-ESS.

Tailoring of the P2P-ESS is against standardisation of the product, which then contributes to higher capital costs of the technology. Nevertheless, in order to assess the potential to enhance the performance of the system by producing specific designs adapted to the installation site, a new section is now presented where ESS will be sized again for each location under consideration. The condition to meet the energy demand of the end user will nevertheless remain in the new analysis. The next section will shed light on how the standarised solution must change from a high GHI site to lower GHI sites.

Table 9
Design parameters for Palermo.

System	Parameter	Unit	Value
PV Solar	Modules per String	-	8
	Strings in Parallel	-	175
	Rated Capacity	kW_{DC}	627.8
	Energy Yield	kWh_{DC}/kW	1731
	Total Module Area	m^2	2842
PEMEC	No Stacks	-	6
	No Cells/Stack	-	112
	Rated Capacity	kW	463
	Rated H_2 Production	Nm^3/h	89.3
Storage	Vessel Volume	L	1208
	Tank Weight	kg	7081
	Shell/Head Thickness	mm	428/157
	Compressor Min/Max Flow Rate	Nm^3/h	9.1/88.6
	Compressor Pressure Ratio	-	13.33
	Compressor Power Rating	kW	12.8
mGT	Rated Output	kW	30
	No Units	-	1
	Rated Electric Eff.	%	26.9

Table 10
Energy balance at different sites when using the system sized for Palermo.

Parameter	Unit	Palermo	Frankfurt	Newcastle upon Tyne
RES Energy	MWh	1086.7	783.4	679.8
mGT Energy	MWh	148.4	151.6	155.0
PEMEC Energy	MWh	(939.5)	(648.9)	(551.7)
Compression Work	MWh	(27.0)	(19.0)	(16.3)
Application Energy	MWh	(262.8)	(262.8)	(262.8)
Surplus Energy	MWh	(32.8)	(23.4)	(20.3)
$[\text{Net } H_2]_{atendyear}$	kg H_2	141	(5247)	(7302)
Seasonal Storage	kg H_2	3125	3125	3125
PV Solar CF	%	18.2	13.2	11.5
LCOH	€/kg H_2	12.72	17.74	21.03
$LCOE_{PV}$	€/kWh	0.0335	0.0425	0.0566
$LCOE_{mGT}$	€/kWh	1.49	2.05	2.42
$\overline{LCOE}$	€/kWh	0.86	1.20	1.44
RTE	%	15.5	-	-

[1] H_2 production minus consumption at the end of the year

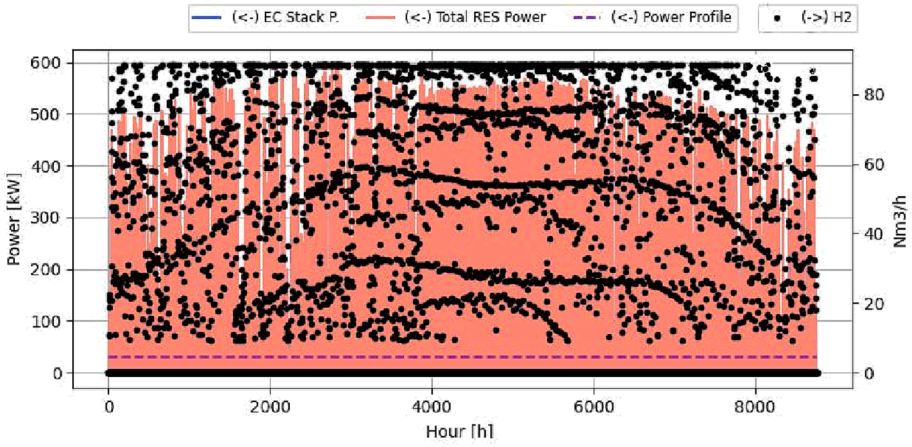

Fig. 8. P2P-ESS Energy Balance for a system designed and operated in Palermo over a complete year (8760 h). For a better understanding, Figs. 9 and 10 show a shorter period of time of the same analysis. Raw data is available for download in CSV format.

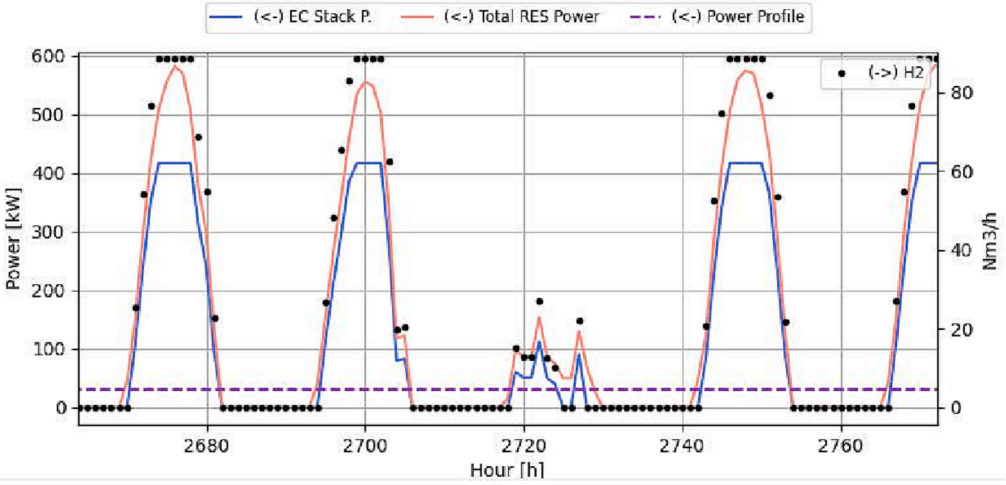

Fig. 9. Close-up of the Power-to-H_2 energy balance for selected days in Fig. 8.Raw data is available for download in CSV format.

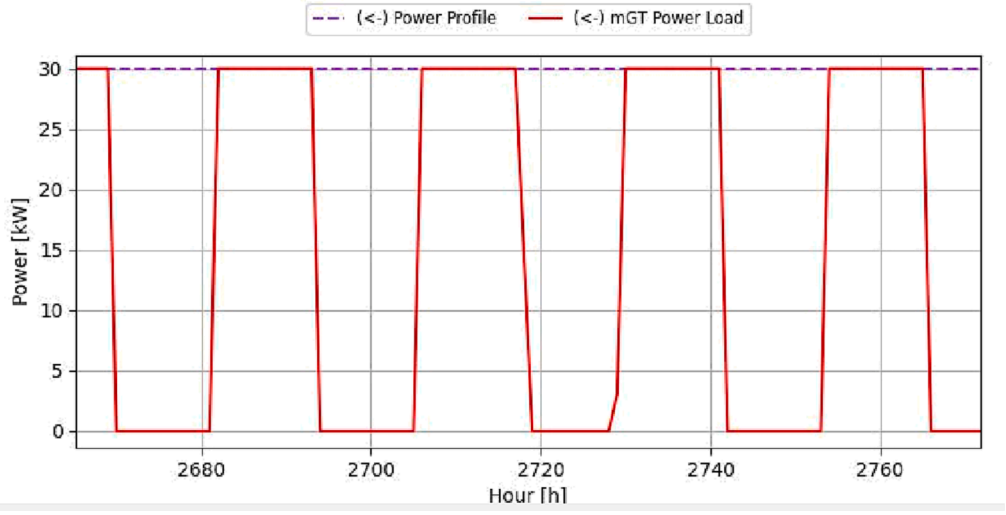

Fig. 10. Close-up of the H_2-to-Power energy balance for selected days in Fig. 8. Raw data is available for download in CSV format.

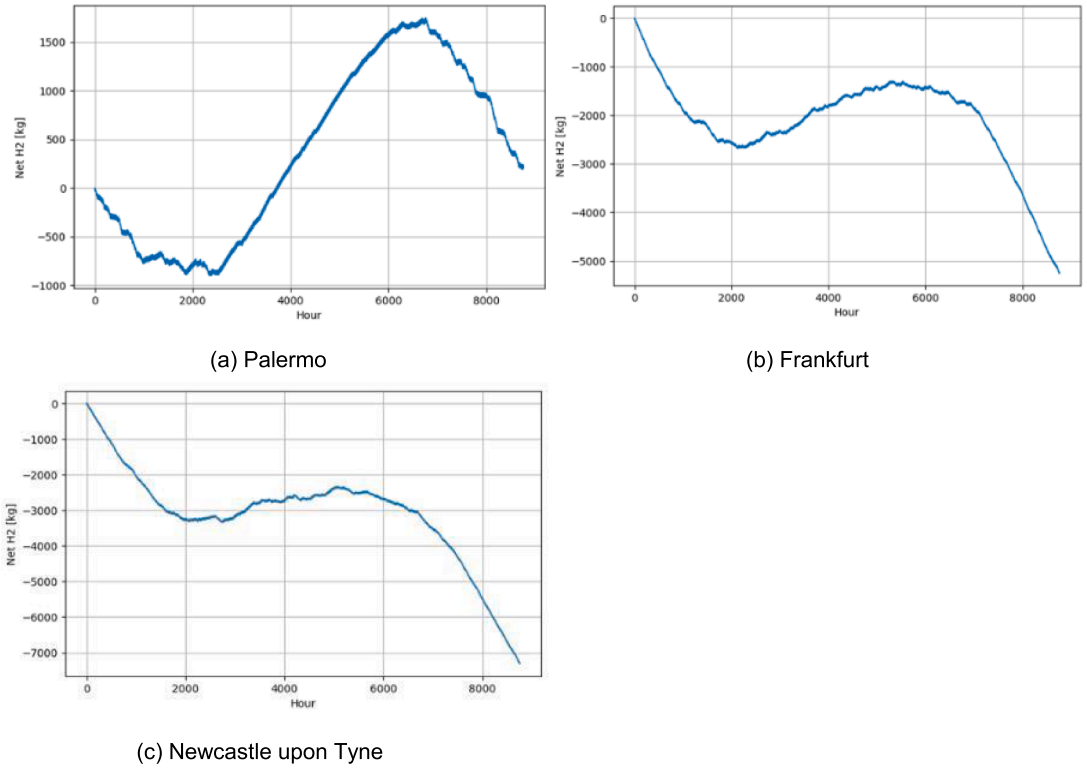

Fig. 11. Hourly net hydrogen balance for three different locations of a P2P-ESS. Design parameters are listed in Table 9.

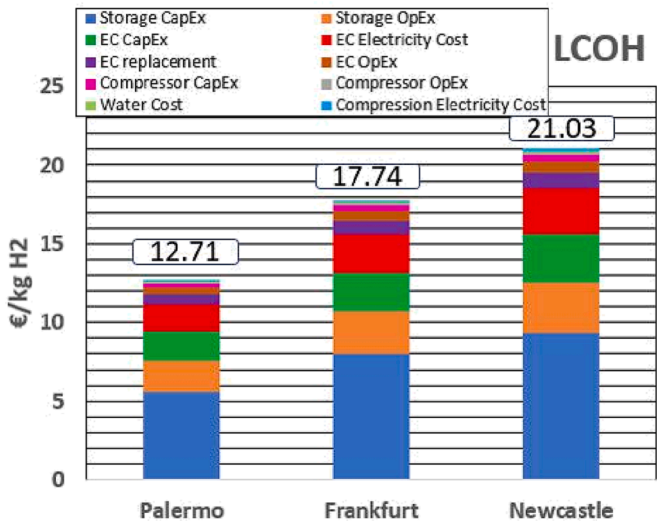

Fig. 12. Breakdown of the Levelised Cost of Hydrogen LCOH of a P2P-ESS installed in Palermo, Frankfurt, and Newcastle upon Tyne. Design parameters and energy balance results are listed in Tables 9 and 10.

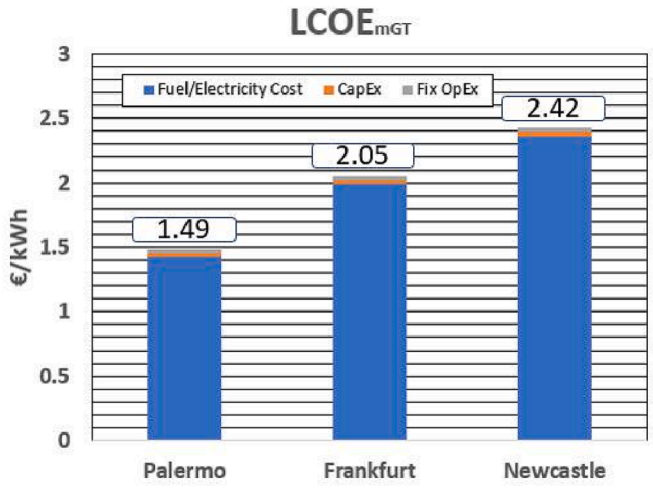

Fig. 13. Breakdown of the Levelised Cost of Energy of the micro gas turbine $LCOE_{mGT}$ of a P2P-ESS installed in Palermo, Frankfurt, and Newcastle upon Tyne. Design parameters and energy balance results are listed in Tables 9 and 10.

4.1. Performance enhancement when producing P2P-ESS designs tailored to the installation site

The previous section examined the possibility to produce a standardised design which could then be used in locations with largely different boundary conditions to those of the reference location. As opposed to this, this section explores the performance enhancement that could be attained if the ESS were tailored to the site in order to obtain a positive net-H_2 at the end of the year as well as the minimum surplus energy such that these quantities were comparable for the three cities considered. The aim of this section is therefore to compare the footprints of each system, LCOH and LCOE.

Table 11 shows the design specifications that are needed in the cities of Palermo, Frankfurt, and Newcastle in order to have a positive net-H_2 balance at the end of the year as well as to minimize the solar energy that is curtailed (i.e., not used by either the end-user directly or the electrolyzer); this curtailed power is termed *Surplus Energy* in the tables. It is worth noting that, as expected, the systems involved in the Power-to-H_2 process are oversized in the Northern locations, with the rated capacity of the solar field/electrolyzer increasing by 37%/41% and 58%/64% for Frankfurt and Newcastle, with respect to Palermo respectively. Regarding footprint, the total module area increases from 2845 m^2 to

Table 11
Tailored design parameters for the locations considered.

System	Parameter	Unit	Palermo	Frankfurt	Newcastle
PV Solar	Modules per String	-	8	8	8
	Strings in Parallel	-	175	240	277
	Rated Capacity	kW_{DC}	628	861	994
	Energy Yield	kWh_{DC}/kW	1731	1248	1082
	Total Module Area	m^2	2842	3898	4499
PEMEC	No Stacks	-	6	10	11
	No Cells/Stack	-	112	95	100
	Rated Capacity	kW	463	655	758
	Rated H_2 Production	Nm^3/h	89.3	126.3	146.2
Storage	Vessel Volume	L	1208	1208	1208
	Tank Weight	kg	7081	7081	7081
	Shell/Head Thickness	mm	428/157	428/157	428/157
	Compressor Min/Max Flow Rate	Nm^3/h	9.1/88.6	12.9/ 125.3	14.9/ 145.1
	Compressor Pressure Ratio	-	13.33	13.33	13.33
	Compressor Power Rating	kW	12.8	18.2	21.0
mGT	Rated Output	kW	30	30	30
	No Units	-	1	1	1
	Rated Electric Eff.	%	26.9	26.9	26.9

3898 m^2 and 4499 m^2, respectively. Overall, this means that footprint of the P2P-ESS increases significantly as latitude increases (in the Northern hemisphere) since this has a strong impact on the energy yield of the PV field.

In addition to the oversizing of the solar field and electrolyzer, Table 12 shows that the seasonal storage becomes more challenging as the amount of hydrogen that needs to be produced during summer and stored for winter is larger for Frankfurt and Newcastle, 5023 kg and 5920 kg of H_2 compared to 3125 kg H_2 for Palermo in the former design case; interestingly, the annual yield of the mGT is almost the same for the 3 cases. This indicates that the mGT is in operation during dark hours most of the time and that the application is powered by the PV panels during sunny hours only; this can also be seen in Figs. 9 and 10. Moreover, the electricity produced by the solar field and that consumed by the electrolyzer are almost the same for the three cases, but the rated output increases when located further up north because the capacity factor of the PV panels and the electrolyzer decreases considerably, affecting the LCOH and LCOE (Table 12).

Table 12
Techno-economic balance of the cities of Palermo, Frankfurt, and Newcastle upon Tyne. Suplementary data is available. Refer to Section Supplementary material.

Parameter	Unit	Palermo	Frankfurt	Newcastle
RES Energy	MWh	1086.7	1074.4	1076.03
mGT Energy	MWh	148.4	149.5	151.2
PEMEC Energy	MWh	(939.5)	(927.9)	(929.3)
Compression Work	MWh	(27.0)	(27.1)	(27.5)
Application Energy	MWh	(262.8)	(262.8)	(262.8)
Surplus Energy	MWh	(32.8)	(33.3)	(35.1)
$[NetH_2]_{atendyear}$	kg H_2	141	106	106
Seasonal Storage	kg H_2	3125	5023	5920
PV Solar CF	%	18.2	13.1	11.3
EC CF	%	23.8	16.9	14.8
LCOH	€/kg H_2	12.72	18.96	22.36
$LCOE_{PV}$	€/kWh	0.0335	0.0425	0.0566
$LCOE_{mGT}$	€/kWh	1.49	2.19	2.57
$\overline{LCOE}$	€/kWh	0.856	1.265	1.497
RTE	%	15.5	15.7	15.9

The levelised costs $LCOH/LCOE_{mGT}$ also increase when changing the reference design conditions, by 49%/47% from Palermo to Frankfurt and 76%/73% from Palermo to Newcastle, respectively. For the $LCOE_{mGT}$ this is mostly driven by the fuel cost (H_2 in this case), as is seen in Fig. 13, whereas the higher LCOH is clearly brought about by the largest storage capacity needed (Fig. 14). If the storage capacity is not considered in the calculation of $LCOH/LCOE_{mGT}$, the costs are $5.0_{€/kgH_2}$ / $0.62_{€/kWh}$, $6.69_{€/kgH_2}$ / $0.81_{€/kWh}$, and $8.07_{€/kgH_2}$/ $0.97_{€/kWh}$ for Palermo, Frankfurt and Newcastle, respectively. LCOH can also be converted into €/MWh, in which case it yields 166.7, 223, and 269 €/MWh($H_{2,LHV}$), respectively. If these costs are compared with the peak price of the *Dutch TTF Gas Futures* [35] in August 2022 −349.9 €/MWh-, the price of H_2 resulting from the analysis is not far from being competitive already.

The discussion presented in this section confirms that latitude plays a very strong role in determining the sizing (footprint) and costs of the subsystems that form the P2P-ESS as well as the amount of seasonal storage. As expected, departing northwise or southwise from the Ecuadorian line has a negative impact on these metrics. If seasonal storage is considered, the hydrogen storage system also becomes larger due to the fewer sun hours during winter, impacting LCOH negatively and, consequently, $LCOE_{mGT}$.

In addition to this, the analysis of energy balance and footprint shows that using a P2P-ESS coupled to a mGT is not practical in an application without grid support, due to the large oversizing of the subsystems and the not-competitive values of LCOE. To overcome this hurdle, the P2P-ESS can be hybridized with other ESSs if grid support is still not available or it can be resized if the system can rely on importing energy from the grid. This latter is, however, not under discussion in this work since the focus is on systems which are off-grid. Therefore, the next section will explore the room for optimization of the system designed for Palermo through the hybridization of a P2P-ESS with a BESS.

5. Performance enhancement through hybridization with battery storage

Installing a P2P-ESS to power an application without grid support leads to high LCOE as well as large footprint of the solar field and electrolyzer system, as already discussed in the foregoing Section 4. Adopting the P2P layout described in Fig. 1 seems therefore impractical.

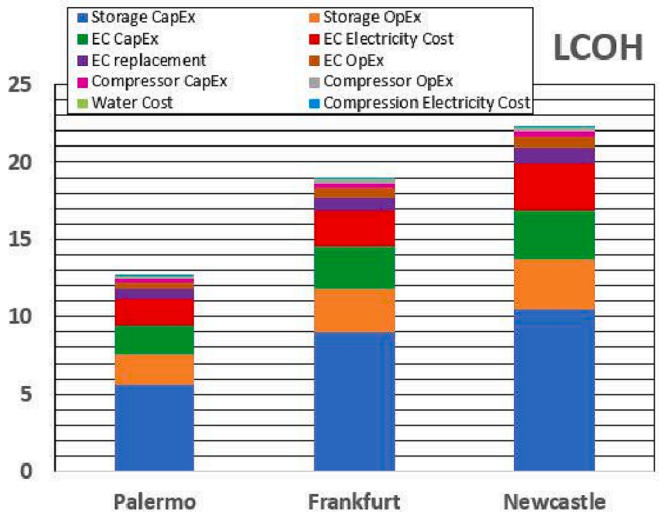

Fig. 14. LCOH breakdown for a P2P-ESS in Palermo, Frankfurt, and Newcastle upon Tyne. Design parameters for each location can be found in Table 11.

Based on this conclusion, this section aims at adopting a new layout that allows making the system more competitive both in terms of lower LCOE and space occupation.

The layout that is now adopted is presented in Fig. 2. This system is applied to the city of Palermo only, since the relative performance enhancement for this location would still be applicable to other cities. The new P2P layout incorporates a BESS that is charged by the PV module during sun hours and discharged when the solar field cannot meet the power demand of the end-user. Hence, charging of the BESS is prioritised over the operation of the electrolyzer, due to the higher RTE and lower cost of the former storage system. The model of the BESS is described in Section 2.2.

An optimization solver is used to solve the techno-economic problem since many trade-offs exist between the different sizing parameters of the systems involved. Thus, multi-objective optimization using the NSGA-II solver [36] is used to calculate a Pareto front based on the following optimization problem:

$$f(1) = \min(LCOE)$$

$$f(2) = \min(\text{Surplus energy})$$

subject to:

$$50 > \text{net } H_2 \text{ (kg)} < 400$$

Minimisation of surplus energy is selected because this is an application without grid support and, therefore, surplus energy would be directly dumped off the system; in addition, minimising this parameter also ensures the lowest footprint of the system. Table 13 shows both the settings of the optimiser and the design space for each input parameter.

Fig. 15 shows the Pareto Front produced by the optimiser with the settings and inputs displayed on Table 13. The main trend shown is that accepting higher surplus energy seems to yield lower LCOE. This is because the capacity factor of the electrolyzer increases as the rated output of the PV module increases and the rated capacity of the electrolyzer decreases, as shown in Fig. 16.

The first consequence of considering the integration of a BESS is therefore a lower LCOE. Nevertheless, the introduction of the BESS has a negative, direct effect on the capacity factor of the electrolyzer and mGT since the BESS is prioritised over the mGT due to its higher round-trip efficiency. Thus, even if the overall trend is a reduction of the $\overline{\text{LCOE}}$, the LCOH and LCOE_{mGT} still increase.

Once the main results have been discussed, a design from the Pareto front is selected, based on the conditions that the maximum surplus energy shall not exceed 30 MWh and that LCOE is the lowest (i.e., the design is on the front); the resulting design is marked in red in Fig. 15. For this design, Table 14 shows the input parameters and Table 15 shows the energy balance and economic metrics. In these two tables, an additional column has been added for the design of the city of Palermo, using the configuration displayed on Fig. 1 and discussed in Section 4.

The reduction in footprint and rated capacity of the PV module and the electrolyzer with respect to the solution without BESS is remarkable.

Table 13
Settings of the optimization problem. P2P-ESS with BESS in Palermo.

	Parameter	Unit	Range
Settings	Population Size	-	100
	No Generations	-	50
	No Offsprings	-	50
	Crossover Rate	-	0.9
	Mutation Rate	-	0.1
Input	No Modules	-	(100, 175)
	Bank Capacity	kWh_{DC}	(120, 400)
	No Stack	-	(3, 6)
	No Cell	-	(80, 120)

Both the footprint and rated output of the PV system are reduced by 32.5% compared to the base case scenario, what adds up to a 45% reduction of the rated capacity of the electrolyzer. This reduction is a consequence of the introduction of the BESS, whose bank capacity is 359 kWh with a duration of 12 h (it must be noted though that, considering the depth of charge/discharge, the actual duration is approximately 8 h). On the other hand, the RTE of the ESS has increased from 15.5% to 25.6% due to the higher RTE of the BESS. In addition, the CF of the mGT is reduced by almost half, from 56.5% to 29.5% (Table 15). Interestingly, even though the $\overline{\text{LCOE}}$ is largely reduced for the optimised solution, 0.69 €/kWh *vs*. 0.86 €/kWh, LCOH has increased from 12.72 €/kg H_2 to 17 €/kg H_2. The reason for this is found in Fig. 17 which shows the breakdown of LCOH for the two ESS layouts considered (for the city of Palermo). It can be seen that the CapEx of storage is much higher now (11.45 €/kg H_2 *vs*. 7.55 €/kg H_2).

As it is seen in Fig. 15, other designs can achieve lower LCOEs. Fig. 16 shows the linear trends for the different inputs considered to minimise the LCOE. These trends show that a higher number of modules/string and a lower capacity of the battery and electrolyzer yield lower LCOE. This comes about because the CF of the electrolyzer increases with decreasing electrolyzer capacity and increasing rated output of the PV system, whilst LCOE_{PV} remains constant due to the moderate effect of economy of scale in the range considered. As a consequence, LCOH is reduced. However, when things proceed in this direction, the amount of surplus energy increases and, since this is an off-grid application, so does the amount of energy dumped off the system. Unexpectedly, even though the LCOE_{BESS} is much lower than the LCOE_{mGT}, the $\overline{\text{LCOE}}$ decreases for decreasing capacities of the battery bank. This is so because when the battery bank capacity increases, the CF of the electrolyzer decreases. At the same time, the consumption of H_2 decreases as more energy is supplied by the battery, while the production of H_2 also decreases but at a much lower rate. This leads to the requirement set on net H_2 at the end of the year (net $H_2 < 400$ kg) not being met; this implies that either the rated output of the solar field or the electrolyzer must be decreased. When this is done, the CF of the electrolyzer increases (yielding lower LCOH) and the same applies to the need for seasonal storage (what yields higher LCOHs). The latter effect is stronger and therefore, the final result is a higher $\overline{\text{LCOE}}$.

It can therefore be concluded that hybridising the P2P-ESS with a BESS would bring down the cost of the LCOE of the application. Additionally, it is important to remark that this is an off-grid application, so energy must be produced onsite and surplus electricity cannot be sold. Furthermore, heat production is not considered in the integration of the ESS with the application; i.e., the techno-economics of the case considered here could be highly improved by having an application with both heat and power demand. These two features, integration of heat and grid integration, will be considered by the authors in further work, possibly with larger-scale systems where economies of scale could also be applied.

6. Conclusions

This paper presents the techno-economic study of a Power-to-Power Energy Storage System (P2P-ESS) designed to meet a continuous demand of 30 kW_e in an off-grid application. To carry out the system analysis, the off-design performance characteristics of the PV installation, the electrolyser, and the micro-gas turbine are considered so as to have more accurate results.

6.1. Specific conclusions

The techno-economic study is carried out with hourly simulations over a year. The first source of energy to satisfy the electric demand of the end-user is solar energy through photovoltaic panels, followed by a battery energy storage system (when available) and, finally, a hydrogen-

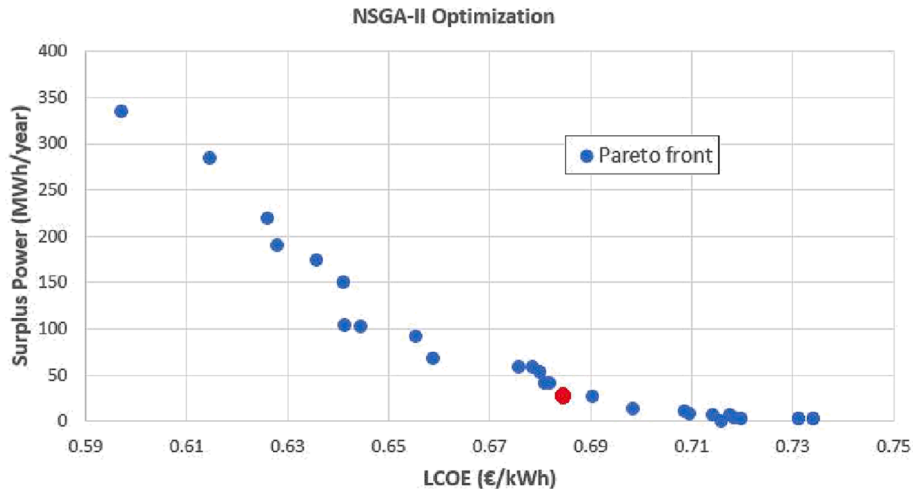

Fig. 15. Pareto front for the global optimization problem. Settings displayed on Table 13.

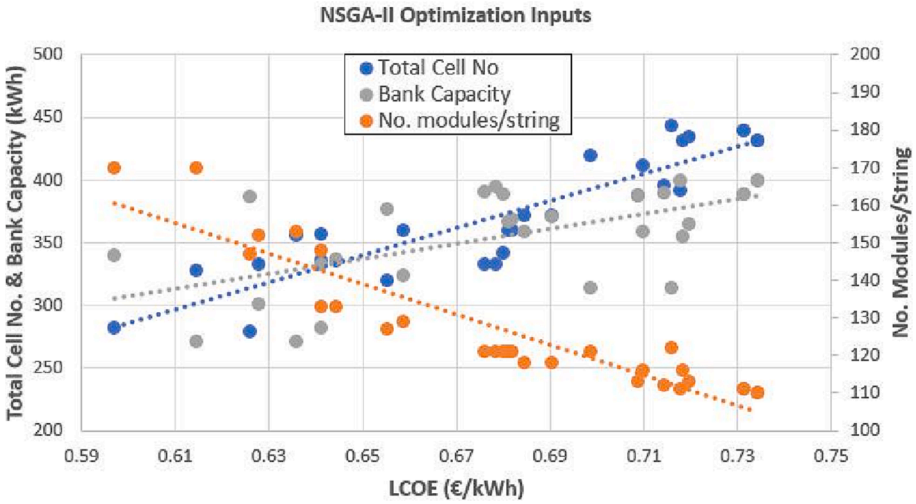

Fig. 16. Input parameters for the Pareto front displayed on Fig. 15 and the linear trends.

fired micro-gas turbine.

In the first part of the analysis, the layout of the P2P-ESS considers a PV installation producing power from solar energy, a PEM electrolyser producing hydrogen that is later stored in high-pressure vessels, and a hydrogen-fired mGT produce power when the renewable energy source is not available (or it is insufficient). The techno-economic performance of this system is studied for three different locations in Europe, selected according to their Global Horizontal Irradiance; Palermo (IT), Frankfurt (DE), and Newcastle upon Tyne (UK).

The following specific conclusions are drawn from the first part of the analysis:

- To satisfy a continuous demand of 30 kW_e in the city of Palermo (IT), a PV installation and PEM Electrolyser with a rated capacitiy of 628 kWp and 463 kWp, respectively, must be employed.
- As much as 3125 kg H_2 would need to be stored in this case, what would imply around 116 high-pressure vessels storing some 22.7 kg H_2 each.
- Redesigning the PV facility and electrolyser for the boundary conditions in Frankfurt and Newcastle leads to an increase in the rated capacity of about 37%/41% and 58%/64% (PV/electrolyser) with respect to the reference case for the city of Palermo. This also leads to an increase in the footprint of the PV facility, which changes from 2845 m^2 in Palermo to 3898 m^2 and 4499 m^2 in Frankfurt and Newcastle, respectively.
- Seasonal storage amounts to 3125 kg H_2, 5023 kg H_2 and 5920 kg H_2 for the cities of Palermo, Frankfurt, and Newcastle, respectively.
- The cost of hydrogen LCOH is strongly influenced by the need for seasonal storage. CapEx and OpEx of the storage system represents about 50% of LCOH. LCOH is approximately 12.72 €/kg H_2, 18.96 €/kg H_2 (49% higher), and 22.36 €/kg H_2 (76% higher) for the cities of Palermo, Frankfurt, and Newcastle. If storage is not accounted for, LCOH drops to less than 6 €/kg in Palermo.
- The cost of H_2 represents more than 95% of the cost of $LCOE_{mGT}$, which is around 1.49 €/kWh, 2.19 €/kWh (47% higher), and 2.57 €/kWh (73% higher) for the cities of Palermo, Frankfurt and Newcastle, respectively. However, the mGT only satisfies a fraction of the total demand for electricity of the end-user, with the average LCOE of the application being 0.856 €/kWh, 1.265 €/kWh, 1.497 €/kWh for the said locations.

The second part of the analysis is focused on the hybridization of the reference (base-case) system with a battery energy storage system. In this case, an optimization process using the NSGA-II solver is incorporated. This optimization is aimed at finding the lowest cost of energy $\overline{LCOE}$ with, simultaneously, the minimum surplus energy (excess solar

Table 14
Design parameters for the optimised design of a system installed in Palermo.

System	Parameter	Unit	Palermo	
			Optimized	Section 4
PV Solar	Modules per String	-	8	8
	Strings in Parallel	-	118	175
	Rated Capacity	kW_{DC}	423	628
	Energy Yield	kWh_{DC}/kW	1731	1731
	Total Module Area	m^2	1916	2842
BESS	Bank Capacity	kWh	359	-
	Bank Power	kW	30	-
	Charged/Discharged Eff.	%	90/90	-
PEMEC	No Stacks	-	4	6
	No Cells/Stack	-	93	112
	Rated Capacity	kW	256	463
	Rated H_2 Production	Nm^3/h	49	89.3
Storage	Vessel Volume	L	1208	1208
	Tank Weight	kg	7081	7081
	Shell/Head Thickness	mm	428/157	428/157
	Compressor Min/Max Flow Rate	Nm^3/h	5/49	9.1/88.6
	Compressor Pressure Ratio	-	13.33	13.33
	Rated Compressor power	kW	7.1	12.8
mGT	Nominal Capacity	kW	30	30
	No Units	-	1	1
	Nominal Electric Eff.	%	26.9	26.9

Table 15
Techno-economic balance of the optimised solution for the city of Palermo. Suplementary data is available. Refer to Section Supplementary material.

Parameter	Unit	Palermo	
		Optimized	Section 4
RES Energy	MWh	732.7	1086.7
mGT Energy	MWh	76.5	148.4
BESS Discharged Energy	MWh	73.5	-
BESS Charged Energy	MWh	(97.2)	-
PEMEC Energy	MWh	(497.0)	(939.5)
Compression Work	MWh	(14.2)	(27.0)
Application Energy	MWh	(262.8)	(262.8)
Surplus Energy	MWh	(26.7)	(32.8)
$[NetH_2]_{atendyear}$	kg H_2	94	141
Seasonal Storage	kg H_2	2558	3125
PV Solar CF	%	18.2	18.2
EC CF	%	22.7	23.8
mGT CF	%	29.5	56.5
LCOH	€/kg H_2	17.0	12.72
$LCOE_{PV}$	€/kWh	0.0335	0.0335
$LCOE_{BESS}$	€/kWh	0.25	-
$LCOE_{mGT}$	€/kWh	2.04	1.49
$\overline{LCOE}$	€/kWh	0.69	0.86
RTE	%	25.6	15.5

energy that is not used to produce electric power). Independent variables in the optimization process are the number of PV modules, capacity of the battery bank, and total number of electrolyser cells. The main conclusions obtained from this study are:

- The selected design on the Pareto front yields an $\overline{LCOE}$ of around 0.69 €/kWh and the total surplus (dumped) energy is around 26.7 MWh/year. This means a 20% $\overline{LCOE}$ reduction with respecto to previous designs without BESS for the city of Palermo.
- Even though the need for seasonal storage decreases from 3125 kg H_2 to 2558 kg H_2 when BESS is incorporated, the capacity factors of electrolyser and mGT decrease and, therefore, the LCOH and $LCOE_{mGT}$ increase from 12.72 to 17 €/kg H_2, and from 1.49 to 2.04 €/kWh, respectively.
- Overall, integrating BESS into P2P-mGT ESS allows to largely reduce the rated capacity of the system and, therefore, the footprint of the PV plant (from 2842 m^2 to 1916 m^2) and the electrolyser. It also increases round-trip efficiency from 15.5% to 25.6%.

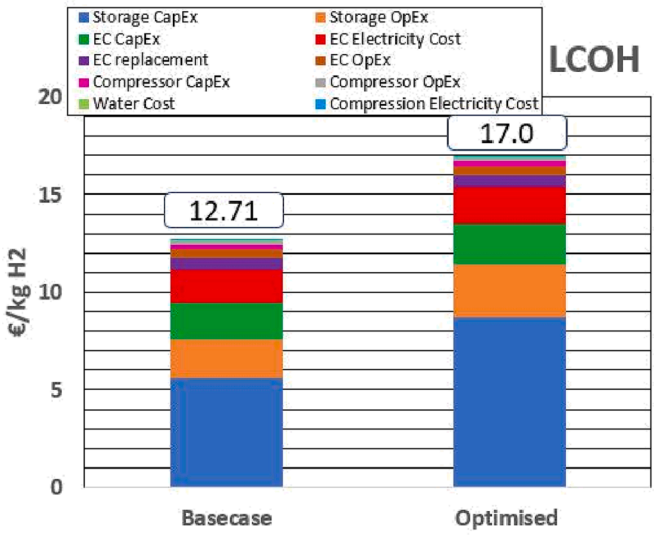

Fig. 17. LCOH for the base-case (Tables 9 and 10) and optimised scenarios (Tables 14 and 15). Results correspond to the city of Palermo.

6.2. General conclusions

The main general conclusions that are drawn from this study are listed below:

1. The storage capacity of an off-grid power-to-power energy storage system (P2P-ESS) cannot be depreciated since H_2 seasonal storage must be accounted.
2. The location of the off-grid P2P-ESS has a very strong impact on the amount of H_2 produced for seasonal storage and on the footprint of the PV plant and storage system.
3. The main parameter affecting the cost of hydrogen (LCOH) for an off-grid power-to-power energy storage system is the CapEx and OpEx of the storage system, followed by the capital cost of the electrolyser and the cost of electricity.
4. The incorporation of a battery energy storage system (BESS) into a P2P-ESS helps to considerably reduce the footprint of the systems as well as the cost of electricity (LCOE).

As a final remark, it becomes clear that the option to use power-to-power energy storage based on micro gas turbines in off-grid applications has evident disadvantages, in particular because of the low round-trip efficiency of the system and, accordingly, the large oversizing that is needed in order to produce hydrogen for seasonal storage. In future works, the authors plan to look into the integration of this energy storage system in applications that are connected to the grid. It is expected that the benefits brought about by economies of scale and by finding tradeoffs between producing electricity and importing electricity from the grid might yield relevant benefits for the end-user, technically and economically. In addition, the option of using hydrogen-fired micro gas turbine might have its applicability when operated for combined heat and power, helping decarbonise those sectors demanding high-grade heat supply.

CRediT authorship contribution statement

Antonio Escamilla: Conceptualization, Methodology, Data curation, Writing – original draft. **David Sánchez:** Conceptualization, Writing – review & editing, Supervision, Project administration. **Lourdes García-Rodríguez:** Supervision, Writing – review & editing, Project administration.

Declaration of Competing Interest

The authors declare that they have no known competing financial interests or personal relationships that could have appeared to influence the work reported in this paper.

Acknowledgment

This work has been developed in the frame of the *Next Generation of Micro Gas Turbines for High Efficiency, Low Emissions and Fuel Flexibility*, NextMGT, which has received funding from the European Union's Horizon 2020 research and innovation programme under Marie Sklodowska-Curie grant agreement No 861079.

Appendix A. Supplementary data

The research article provides access to the results of the analyzed cases, which are available in the form of three separate *.csv* files. These files include data related to the Palermo (with and without BESS), Frankfurt, and Newcastle upon Tyne techno-economic cases. Each file contains information on the energy balance of the power-to-power system for every hour of a year, what include the following parameters: application power demand (kWh), PV plant power production (kWh), EC stack power consumption (kWh), EC BoP power consumption (kWh), mGT power production (kWh), BESS State-of-Charge (kWh), and H_2 production (Nm^3/h). Supplementary data associated with this article can be found, in the online version, athttps://doi.org/10.1016/j.ecmx.2023.100368.

References

[1] Cells F, Undertaking HJ. Hydrogen roadmap europe: A sustainable pathway for the european energy transition (Jan. 2019). URL: https://www.fch.europa.eu/publications/hydrogen-roadmap-europe-sustainable-pathway-european-energy-transition.
[2] FCHEA. Road map to a us hydrogen economy (Dec. 2020).
[3] Hydrogen, F.C.S. Council, The strategic road map for hydrogen and fuel cells (Mar. 2019).
[4] G. o. C. Ministry of Energy, National green hydrogen strategy (Nov. 2020). URL: https://energia.gob.cl/sites/default/files/national_green_hydrogen_strategy_-_chile.pdf.
[5] E. Commission, fit for 55: delivering the eu's 2030 climate target on the way to climate neutrality. URL: https://www.consilium.europa.eu/en/policies/green-deal/fit-for-55-the-eu-plan-for-a-green-transition/.
[6] Deb K, Pratap A, Agarwal S, Meyarivan T. A fast and elitist multiobjective genetic algorithm: Nsga-ii. IEEE Trans Evol Comput 2002;6(2):182–97. https://doi.org/10.1109/4235.996017.
[7] Escamilla A, Sánchez D, García-Rodríguez L. Assessment of power-to-power renewable energy storage based on the smart integration of hydrogen and micro gas turbine technologies. Int J Hydrogen Energy 2022;47(40):17505–25. https://doi.org/10.1016/j.ijhydene.2022.03.238.
[8] Heymann F, Rüdisüli M, vom Scheidt F, Camanho AS. Performance benchmarking of power-to-gas plants using composite indicators. Int J Hydrogen Energy 2022;47(58):24465–80. https://doi.org/10.1016/j.ijhydene.2021.10.189.
[9] Loisel R, Baranger L, Chemouri N, Spinu S, Pardo S. Economic evaluation of hybrid off-shore wind power and hydrogen storage system. Int J Hydrogen Energy 2015;40(21):6727–39. https://doi.org/10.1016/j.ijhydene.2015.03.117.
[10] Skordoulias N, Koytsoumpa EI, Karellas S. Techno-economic evaluation of medium scale power to hydrogen to combined heat and power generation systems. Int J Hydrogen Energy 2022;47(63):26871–90. https://doi.org/10.1016/j.ijhydene.2022.06.057.
[11] Crespi E, Colbertaldo P, Guandalini G, Campanari S. Design of hybrid power-to-power systems for continuous clean pv-based energy supply. Int J Hydrogen Energy 2021;46(26):13691–13708, european Fuel Cell Conference &s066amp;) Exhibition 2019. doi: 10.1016/j.ijhydene.2020.09.152.
[12] Zhang Y, Campana PE, Lundblad A, Yan J. Comparative study of hydrogen storage and battery storage in grid connected photovoltaic system: Storage sizing and rule-based operation. Appl Energy 2017;201:397–411. https://doi.org/10.1016/j.apenergy.2017.03.123.
[13] Shahid Z, Santarelli M, Marocco P, Ferrero D, Zahid U. Techno-economic feasibility analysis of renewable-fed power-to-power (p2p) systems for small french islands. Energy Convers Manage 2022;255:115368. https://doi.org/10.1016/j.enconman.2022.115368.
[14] Parra D, Walker GS, Gillott M. Modeling of pv generation, battery and hydrogen storage to investigate the benefits of energy storage for single dwelling. Sustain Cities Soc 2014;10:1–10. https://doi.org/10.1016/j.scs.2013.04.006.
[15] C. National Renewable Energy Laboratory. Golden, System advisor model version 2020.11.29 (sam 2020.11.29). URL: https://sam.nrel.gov.
[16] C. National Renewable Energy Laboratory. Golden, Pysam version 2.2.0. URL: https://github.com/nrel/pysam.
[17] H. T, P.P. I, G.A. A, PVGIS 5: Internet tools for the assessment of solar resource and photovoltaic solar systems (2017).
[18] DiOrio N, Dobos A, Janzou S, Nelson A, Lundstrom B. Technoeconomic modeling of battery energy storage in sam. doi:10.2172/1225314. URL: https://www.osti.gov/biblio/1225314.
[19] Exergy Analysis of Green Power-to-Hydrogen Chemical Energy Storage, Vol. Volume 4: Cycle Innovations; Cycle Innovations: Energy Storage of Turbo Expo: Power for Land, Sea, and Air. doi:10.1115/GT2022-82107.
[20] Colbertaldo SCP, Laura S. Zero-dimensional dynamic modeling of pem electrolyzers. Energy Proc 2017;142:1468–1473, proceedings of the 9th International Conference on Applied Energy. doi: 10.1016/j.egypro.2017.12.594.
[21] Liso V, Savoia G, Araya SS, Cinti G, Kaer SK. Modelling and experimental analysis of a polymer electrolyte membrane water electrolysis cell at different operating temperatures. Energies 11(12). doi:10.3390/en11123273.
[22] Online Companion Guide to the ASME Boiler and Pressure Vessel Codes: Criteria and Commentary on Select Aspects of the Boiler; Pressure Vessel Codes, ASME Press, 2020. doi:10.1115/1.861981.
[23] Mokhatab S, Poe WA. Chapter 11 – natural gas compression. In: Mokhatab S, Poe WA, editors. Handbook of Natural Gas Transmission and Processing. 2nd ed. Boston: Gulf Professional Publishing; 2012. p. 393–423. https://doi.org/10.1016/B978-0-12-386914-2.00011-X.
[24] Razak A. Industrial Gas Turbines: Performance and Operability, Industrial Gas Turbines: Performance and Operability. Woodhead Pub; 2007. URL: https://books.google.es/books?id=W_jXzgEACAAJ.
[25] I.R.E.A. (IRENA), Renewable power generation costs in 2021, Tech. rep. (07 2022).
[26] P.N.N.L. (PNNL), 2020 grid energy storage technology cost and performance assessment, Tech. rep. (12 2020).
[27] Cole W, Frazier AW, Augustine C. Cost projections for utility-scale battery storage: 2021 update, Tech. rep. (6 2021).
[28] IRENA. Green hydrogen cost reduction (2020). URL: https://irena.org/publications/2020/Dec/Green-hydrogen-cost-reduction.
[29] T.B. et al., dena-leitstudie integrierte energiewende: Impulse für die gestaltung des energiesystems bis 2050, Tech. rep. (07 2018).
[30] Khan M, Young C, MacKinnon C, Layzell D. Technical brief: The techno-economics of hydrogen compression, Tech. Rep. 1 (10 2021).
[31] H2a: Hydrogen analysis production models, accessed: 2022–04-21. URL: https://www.nrel.gov/hydrogen/h2a-production-models.html.
[32] Tractebel, Engie, Hinicio, Study on early business cases for h2 in energy storage and more broadly power to h2 applications, Tech. rep. (07 2017).
[33] Darrow K, Tidball R, Wang J, Hampson A. Catalog of chp technologies, Tech. rep., funded by the U.S. Environmental Protection Agency and the U.S. Department of Energy (09 2017).
[34] Cuomo MA, Kool ED, Reddy BV, Rosen MA. Economic and environmental analyses of multi-generation renewable energy system for dairy farms. Eur J Sustain Develop Res 6. doi:https://doi.org/10.21601/ejosdr/11397.
[35] Ice endex: Dutch ttf gas futures, accessed: 2022–09-15. URL: https://www.theice.com/products/27996665/Dutch-TTF-Gas-Futures/data.
[36] Deb K, Pratap A, Agarwal S, Meyarivan T. A fast and elitist multiobjective genetic algorithm: Nsga-ii. IEEE Trans Evol Comput 2002;6(2):182–97. https://doi.org/10.1109/4235.996017.